DESIGN ANALYSIS OF A ROTARY-TYPE MAGNETIC COOLER

Celik S.* and Ekren O.
*Author for correspondence
Department of Mechanical Engineering,
Southern Illinois University Edwardsville,
Edwardsville, IL, 62026,
U.S.A.,
E-mail: scelik@siue.edu

ABSTRACT

Heat flow across the disc of a rotary-type magnetic refrigerator was studied employing volumetric energy generation as a result of which the magnetocaloric material cools down. Gadolinium was selected as the magnetocaloric material due to its competitive cost and magnetocaloric effect. A 90° annular sector of gadolinium was implemented to the rotating disk and simulations were conducted based on the changing geometric values. Three different geometries of disk-magnetocaloric material assembly were studied where R_i = 5, 10, 15 mm, and R_o = 10, 15, 20 mm, respectively. Temperature behavior of the gadolinium was observed at varied disc geometries. Analysis was conducted for both the top surface and the midplane of the rotating disk, accounting for both convective and conductive heat transfer. A Nusselt-Rayleigh relation was obtained for the disks. The cycle was considered to have four processes which are magnetization process simulated by volumetric energy generation, adiabatic 90° rotation to cold side heat exchanger, surface heat flux to the magnetocaloric material within the heat exchanger, and 270° rotation accompanied by convective heat transfer back to the magnetic field, hence completing one cycle. It was observed that the gradient between steady-state temperature and the equilibrium (room) temperature decreases with decreasing gadolinium-to-disk area ratio. Conductive heat transfer through the thickness of the disk was not found to be significant compared to the convective heat transfer through the top surface.

NOMENCLATURE

B	[T]	Magnetic induction
c_p	[J/kgK]	Specific heat
COP	[-]	Coefficient of performance
D	[mm]	Diameter
h	[W/m^{2}K]	Convection heat transfer coefficient
H	[A/m]	Magnetic field
k	[W/mK]	Thermal conductivity
M	[A/m]	Magnetization
Nu	[-]	Nusselt number
Pr	[-]	Prandtl number
R	[mm]	Radius
Ra	[-]	Rayleigh number
Re	[-]	Reynolds number
S	[J/K]	Entropy
T	[K]	Temperature
t	[mm]	Thickness

Special Characters

$\mathcal{E}$	[-]	Porosity
μ_0	[Tm/A]	Permeability
ρ	[kg/m^3]	Density
θ	[degree]	Rotation angle
υ	[m^2/s]	Kinematic viscosity
ω	[rad/s]	Angular velocity

Subscripts

elec	Electronic
i	Inner
o	Outer
lat	Lattice
mag	Magnetic
tot	Total

INTRODUCTION

Magnetic cooling is based on the magnetocaloric effect. When a magnetocaloric material (*MCM*) is placed in an external magnetic field the magnetic atom dipoles align, which would decrease the magnetic entropy of the material. In response to this potential decrease in magnetic entropy the temperature of the material increases in order to maintain its total entropy because a decrease in entropy is impossible due to the second law of thermodynamics. If the thermal energy is subsequently removed by a heat exchanger, when the magnetic field is removed the magnetic dipoles return to their original state of misalignment and the temperature in the material decreases to one below the original temperature before the magnetic field was applied. This is the basis of the magnetic refrigeration cycle. There are two types of magnetic refrigerators currently. One of these is the reciprocating-type magnetic refrigerator where fluid is alternately pushed back and forth between an array of plates that are made of a *MCM*. An electromagnet is turned off and on cyclically in order to alternately remove energy from the *MCM* while the magnetic field is on, and then to dump heat into the *MCM* while the magnet is turned off. The other type of magnetic cooling systems is the rotary-types. These systems operate by taking a piece of *MCM* and placing it on a disk which is rotating relatively compared to a fixed permanent magnet. As the disk is rotated the *MCM* moves under the permanent magnet which is coupled with a hot side heat exchanger, then away from the magnet moving into the cold side heat exchanger which then absorbs heat from the system into the disk, and the process is repeated on a cyclic manner.

BACKGROUND

Magnetocaloric Effect Modeling

While magnetic field applied temperature of magnetic material is increased, this is known as magnetocaloric effect. The total entropy of a magnetic material consists of three main components: S_{mag}, S_{lat} and S_{elec}.

$$S_{tot}(B,T) = S_{mag}(B,T) + S_{lat}(T) + S_{elec}(T) \qquad (1)$$

The electron entropy is disregarded since its effect is quite small comparing to the others. Figure 1 shows the two basic processes of the magnetocaloric effect when a magnetic field is applied or removed in a magnetic system: the isothermal process, which leads to an entropy change, and the adiabatic process, which yields a temperature variation.

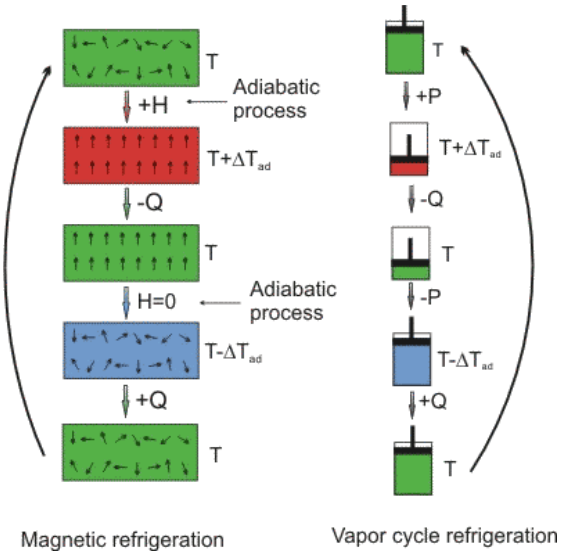

Figure 1 A principle view of magnetic cooling cycle [1]

In the process, after magnetization of a magnetic material by applying magnetic field molecular moments are forced to line up in the same direction and decreases the magnetic entropy. While the total entropy is constant, the reduction in the magnetic entropy then results an increase in the material's lattice entropy. Increase of lattice entropy results an adiabatic increase in magnetic material temperature. During demagnetization the molecules tend to be arranged randomly and increase the magnetic entropy. While the total entropy is constant, the increasing in the magnetic entropy then results in a decrease in the material's lattice entropy and temperature.

The way that the magnetocaloric effect works is that when a magnetic field is applied atomic dipoles in the material align themselves uniformly with the magnetic field. This effect alone would cause the entropy of the material to decrease however due to the second law of thermodynamics this is impossible so the individual atoms respond by vibrating faster which is shown in the form of an increase in temperature of the *MCM*. Quantum mechanics has two functions that can be used to model the effect of the dipoles aligning themselves in the magnetic field. The first is the Langevin function. This function is a simplification of the more general Brillouin function and is obtained by assuming that all of the magnetic dipoles in a substance are free to rotate and there is no resistive torque on the magnetic dipole in the presence of a magnetic field. The Brillouin function is more complicated but does not make this same simplification. Bingfeng *et al.* [2] compared the two functions and found approximately 2-3% error at the Curie point for pure Gd. This indicated that it is possible to use the simplified function to estimate the adiabatic temperature change of Gd at different magnetic field strengths and temperatures. Peterson *et al.* [3] used the Brillouin function to estimate the magnetocaloric effect of Gd in their model.

MCM and the Heat Exchanger

There are several magnetocaloric material geometries used in the literature. One of these is the packed bed type regenerator which is a compartment of sphere shaped *MCM* particles that create a porous bed. The particle sizes as reported by Zimm *et al.* [4] range from 425-500 μm diameters. The Nusselt number that was proposed for this type of packed bed of spheres is:

$$Nu = \frac{hD}{k}\frac{\varepsilon}{1-\varepsilon} = \left(.5\,\mathrm{Re}^{1/2} + .2\,\mathrm{Re}^{2/3}\right)\mathrm{Pr}^{1/3} \qquad (2)$$

where D is the particle diameter, k is the thermal conductivity of the refrigerant and ε is the porosity of the packed bed. Another issue with this type of packed bed geometry in a rotating magnetic refrigerator is the entrained fluid. This is the fluid that stays in the packed bed of *MCM* as it rotates around between the different cycles (magnetization, cold side heat exchanger, hot-side heat exchanger, demagnetization). This phenomenon causes large thermal losses and needs to be considered whenever this type of geometry is chosen. Engelbrecht *et al.* [5] considered the entrained fluid by adding an additional term in the governing equation of the numerical model to account for the energy that is stored in the fluid. Siddikov *et al.* [6] developed a 1D transient numerical model of the active magnetic regenerator (AMR) with backed bed magnetic material and obtained adiabatic temperature change and specific heat of Gadolinium as an approximated function of temperature and magnetic induction. Sarlah *et al.* [7] designed a porous honeycomb regenerator and realized numerical analysis of different magnetocaloric material at different arrangements. Petersen *et al.* [8] compared 1D and 2D AMR models. Sarlah and Poredos [9] in another study introduced a dimensionless model to determine the heat transfer coefficient of the regenerator and the operation of the AMR refrigerator (AMRR). Roudaut *et al.* [10] developed a 1D transient numerical code of an AMR. The mean field theory was used to evaluate the magneto-caloric properties of Gadolinium. Eriksen *et al.* [11] investigated design and construction aspects of a high frequency rotary AMR system. In this study, they reached temperature span values of 25 K and 20.5 K for the unloaded and 100 W of cooling load cases, respectively. Lozano *et al.* [12] investigated an AMR type magnetic refrigerator prototype

with packed sphere gadolinium. At 1.24 T with permanent magnets and a 200 W load, 18.9 K was achieved.

The other main type of *MCM* geometry in literature is an array of flat parallel plates or microchannels in which the fluid is pushed back and forth through the plate array as needed in order to alternately cool and heat the refrigerant with the *MCM*. This type of magnetic refrigeration system is known as the reciprocating type. Chen *et al.* [13] both experimentally and numerically investigated a reciprocating AMR system with microchannels. Vasile *et al*. [14] studied a reciprocating system where the heat transfer was calculated by considering two flat parallel plates that were very close together in order to determine the Nusselt number. The experimental values for the heat transfer coefficient, h, were reported to be ranging from 11000 to 20000 W/m^{2}K for their microchannel setup.

The main advantage for the porous or packed bed design is it gives a large heat transfer coefficient between the *MCM* and the working fluid but this additional heat transfer is balanced by the large pressure losses through the packed bed that the microchannel design does not have. The working fluid selected is mostly water, water-glycol mixture, or air in these applications. There are studies where helium is used as the refrigerant in order to prevent oxidation of the Gd spheres [15].

NUMERICAL MODEL

The model used is a rotary-type, solid disk that has an angular sector that is made of Gd. A schematic of the system is given in Figure 2 where θ is the angle of the Gd sector, t is the thickness of the disk, R_0 is the outer radius of the disk, and R_i is the inner radius of the Gd sector.

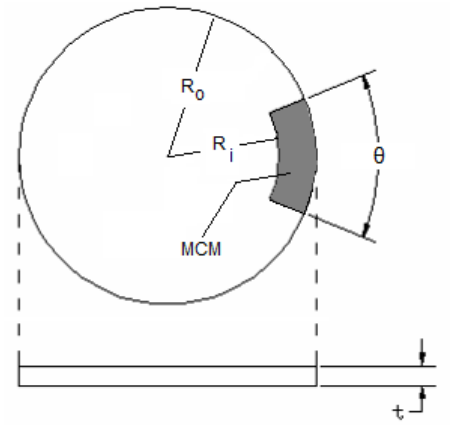

Figure 2 Rotating disk and *MCM* geometry

Three different geometric cases were solved with the numerical model. These scenarios are listed in Table 1. Properties of Gd metal used as the *MCM* are given in Table 2.

Table 1 Geometric values for the simulated disks

Case	R_o (mm)	R_i (mm)	t (mm)	θ (°)
1	100	50	5	90
2	150	100	5	90
3	200	150	5	90

Table 2 Properties of gadolinium

Density, ρ	7.89 g/cm^3
Specific heat, c_p	240 J/kg·K
Thermal conductivity, k	10.6 W/m·K

Solutions to the numerical model were obtained using a fully implicit discretization of the governing energy equations. A convergence tolerance of 0.005 K was selected along with a relaxation factor of 5. Thermal behaviour of the solid matrix was perceived using second order upwind scheme to minimize artificial diffusion. Energy equation for the *MCM* can be written as:

$$\rho_{MCM}\frac{\partial u_{MCM}}{\partial t} = \mu_0 H\frac{\partial M}{\partial t} - \frac{Nu_d k_f}{D_h}(T_{MCM} - T_f) \qquad (3)$$

where the terms are; rate of change of stored energy in the *MCM*, magnetic work, and the heat transfer from the disk to the fluid, per unit area, respectively. Convective heat transfer analysis from the disk to the air during the final process of 270° rotation back to the magnetization phase showed that free convection dominates forced convection due to a low angular velocity of 1rpm. This was verified by

$$Gr/\mathrm{Re}^2 >> 1 \qquad (4)$$

for all three cases. Hence, pure free convection was considered with the correlation for a thin, horizontal disk [16]

$$Nu_d = 0.9724\,Ra^{0.194} \qquad (5)$$

Validation of the simulations was achieved through comparison to a sample natural convection problem from a horizontal [17] and a vertical [18] disk. All cases were studied over four processes through a single revolution of the magnetic cooling cycle. The magnetization process (1-2) was simulated along with a volumetric energy generation (2-3) which acts to cool down the *MCM* by 10K in a certain amount of time through the hot side heat exchanger (*HHX*). The third process (3-4) is the 90° rotation of the disk from underneath the magnet to the cold side heat exchanger (*CHX*). During this step it was assumed that there is no heat transfer from the disk to its surroundings (adiabatic quarter rotation). As the *MCM* reached the cold side heat exchanger, a surface heat flux boundary condition was imposed to simulate the transfer of energy from the system to the *MCM*. The last process (4-1) of the cycle is the rotation of the disk from the cold side heat exchanger back to the magnet which translates to 270° rotation of the disk. Schematic of the rotary mechanism and the T-s diagram can be seen in Figure 3.

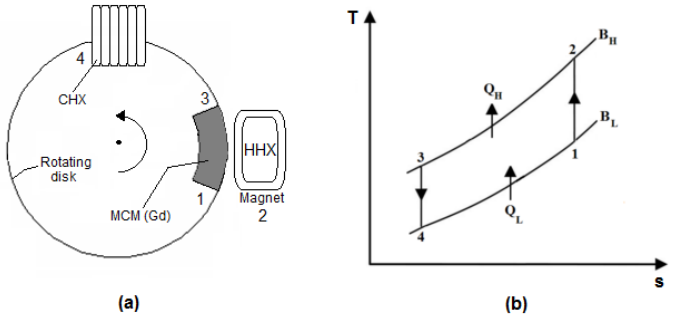

Figure 3 (a) Rotary-type magnetic cooler simulation setup, (b) T-s diagram for the Brayton cycle with two isomagnetic and two adiabatic processes

Coefficient of performance (COP) of the system can be expressed in terms of the net work of the cycle, W_{net}, and the cooling energy, Q_L.

$$W_{net} = \mu_0 \left(\int_1^2 M dH_0 + \int_3^4 M dH_0 \right) = Q_H - Q_L \quad (3)$$

$$W_{net} = \int_2^3 T ds - \int_4^1 T ds \quad (4)$$

$$COP = \frac{Q_L}{W_{net}} \quad (5)$$

The system was simulated to have 40W of cooling capacity for all three cases. Hence, for changing surface areas of the *MCM*, different heat fluxes for the *CHX* were calculated. Table 3 lists the calculated heat fluxes for the three cases studied. Required energy to cool the Gd sector was calculated by the mass and specific heat of the Gd slice, and the assigned temperature difference of 10K.

Table 3 Calculated CHX heat fluxes for three cases

Case	CHX heat flux (kW/m^2)	MCM area (m^2)	MCM volume (m^3)	Cooling capacity (W)
1	3.0	0.0063	1.47E-5	18.8
2	3.0	0.0104	2.45E-5	31.2
3	3.0	0.0145	3.43E-5	43.6

RESULTS

Heat transfer results from the simulation were compared to existing data [16-18] in literature. Nusselt number was plotted as a function of Raleigh number for illustration of this comparison, as given in Figure 4. Results are in close agreement with prior data for a horizontal disk which is the case in the present simulation. A vertical disk case from literature [18] was also plotted to see the difference with changing orientation. COP and Nusselt number were also plotted with respect to the *MCM* volume for each case studied. The relation can be seen in Figure 5.

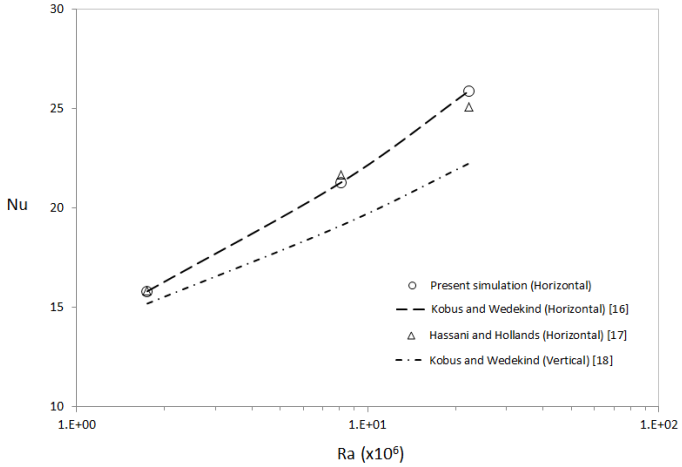

Figure 4 Comparison of the heat transfer results with other existing data

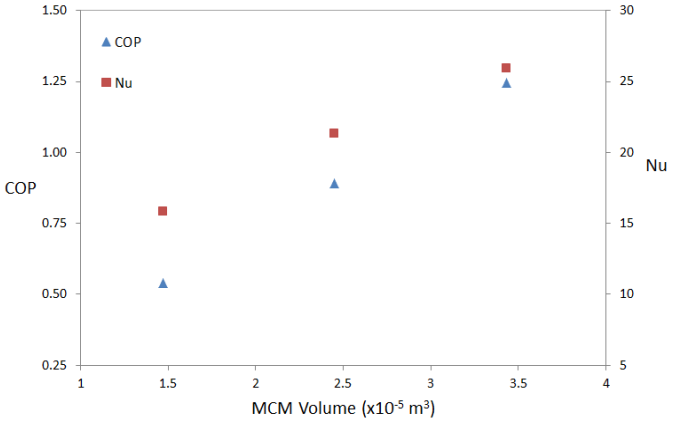

Figure 5 COP and Nu values for different gadolinium (MCM) amounts used in three cases

Surface temperature variation of the gadolinium material (*MCM*) implemented into the rotating disk at varied geometric properties are illustrated in Figure 6 for the first revolution of the first case as an example, and in Figures 7-9 for multiple revolutions of the disks in all cases.

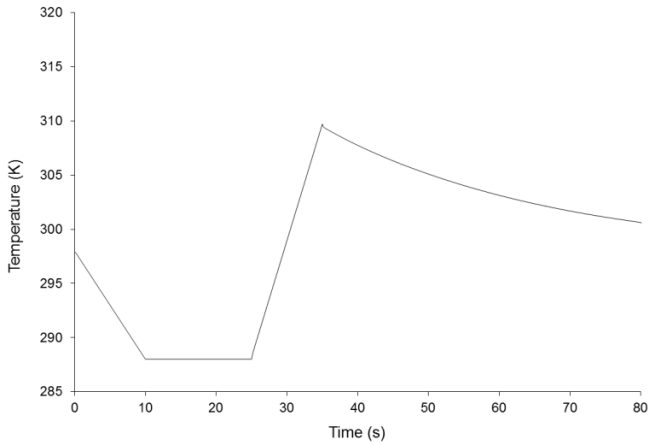

Figure 6 Case 1 (R_0 = 100 mm, R_i = 50 mm), 1st revolution

Each cycle consists of 10 seconds waiting per heat exchanger with 2π/min rotational speed outside the heat exchangers, yielding a whole cycle of 80 seconds. For this process, a convection boundary condition was set where the ambient temperature was assumed to be 298 K corresponding to room temperature.

Figures 7-9 contain a *Max Delta T* term which is defined as the difference between the maximum steady-state temperature and the initial temperature where initial temperature was constant for all cases to be 298K which is room temperature. It is desired that that this temperature difference is minimized to lessen the external heat transfer during the rotations. As can be seen in the figures, case 3 yielded the most appropriate geometric design in terms of the temperature gradient between the disk and the surroundings. This volume was sufficient to accept 40 watts of heat from the *CHX* while maintaining its maximum cycle temperature very close to room temperature which is the optimal condition for entering the magnetic field.

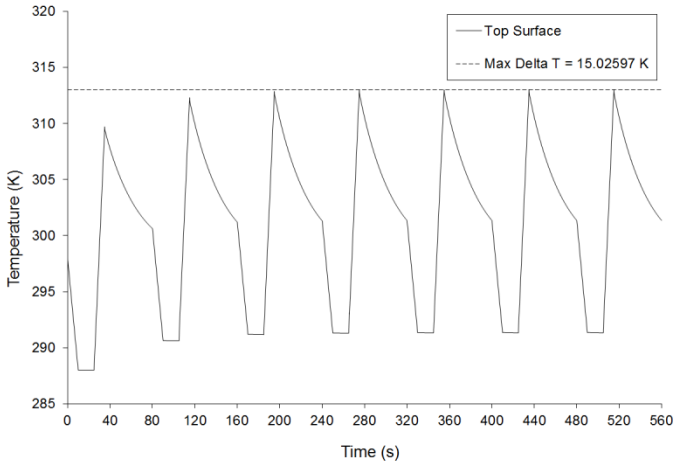

Figure 7 Case 1 (R_0 = 100 mm, R_i = 50 mm), top surface temperature variation for 7 revolutions

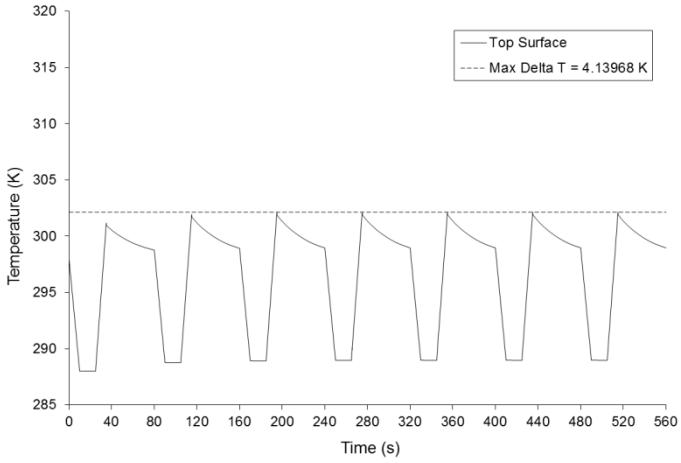

Figure 8 Case 2 (R_0 = 150 mm, R_i = 100 mm), top surface temperature variation for 7 revolutions

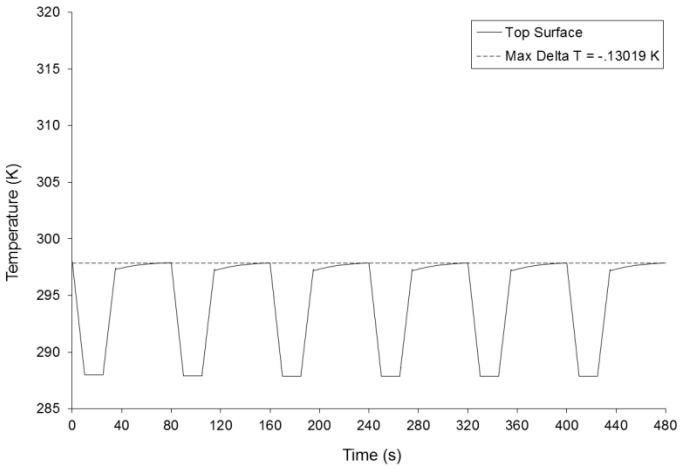

Figure 9 Case 3 (R_0 = 200 mm, R_i = 150 mm), top surface temperature variation for 6 revolutions

Besides surface temperature analysis, temperature variations at the midplane of the disks were also obtained to observe the conduction effects through the thickness of the rotating disk. These plots are given in Figures 10-12 representing each case.

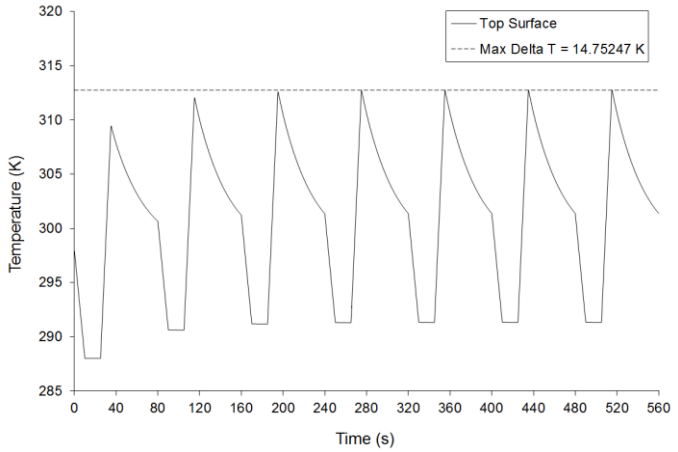

Figure 10 Case 1 (R_0 = 100 mm, R_i = 50 mm), midplane temperature variation for 7 revolutions

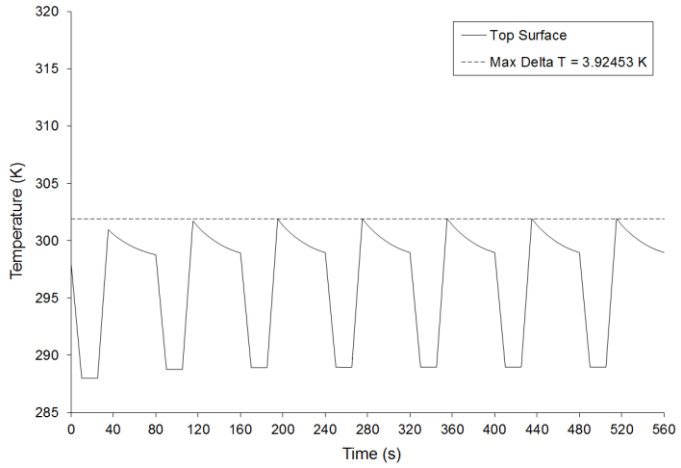

Figure 11 Case 2 (R_0 = 150 mm, R_i = 100 mm), midplane temperature variation for 7 revolutions

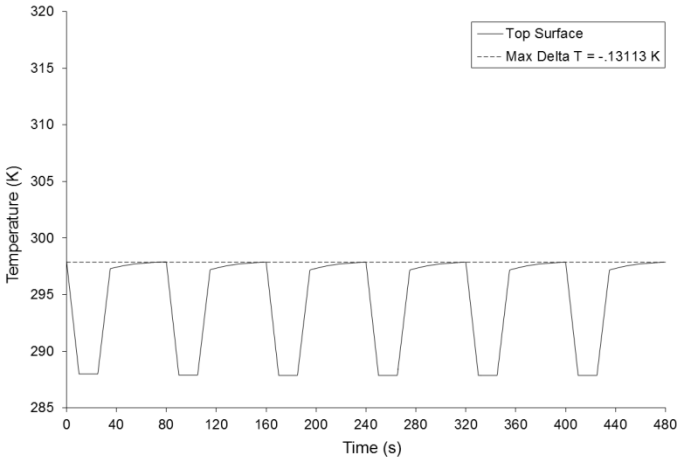

Figure 12 Case 3 (R_0 = 200 mm, R_i = 150 mm), midplane temperature variation for 6 revolutions

CONCLUSION

Magnetocaloric materials implemented on a rotating disk as a sector with a given angle can be characterized by their thickness, speed of the rotating disc and the efficiencies of the cold-side and hot-side heat exchangers which act as heat sources and heat sinks, respectively. This study used a 90° annular gadolinium sector embedded into a 5 mm-thick disk rotating at an angular speed of 2π/min.

Validation of the simulation was performed by comparison of results to prior theoretical and experimental work. COP and Nusselt number as a function of the *MCM* volume were obtained. The gradient between steady-state temperature and the initial (room) temperature was found to be a function of Gd-to-disk area ratio. This temperature difference reduced with decreasing ratio of Gd amount over the disk. As minimizing this temperature difference is critical for maintaining energy, case 3 with R_o=200mm and R_i=150mm yielded the most effective results. Conductive heat transfer through the thickness of the disk was not found to be significant compared to the convective heat transfer through the top surface. Highest temperature difference between the top surface and midplane was found to be ~0.25K. This is due to comparatively low thermal conductivity of the magnetocaloric material.

The simulations performed in this study enable the prediction of the maximum possible cooling capacity of rotary-type magnetic cooling systems with given operating conditions and geometric properties.

REFERENCES

[1] Burdyny T., Simplified Modeling of Active Magnetic Regenerators, *Master of Science Thesis, Mechanical Eng. Dept., University of Victoria*, 2010.

[2] Bingfeng Y. and Yan Z., Research on performance of regenerative room temperature magnetic refrigeration cycle, *International Journal of Refrigeration*, vol. 29, 2006, pp.1348-1357.

[3] Peterson T.F. and Pryds N., Two-dimensional mathematical model of a reciprocating room-temperature Active Magnetic Refrigerator, *International Journal of Refrigeration*, vol. 30, 2007, pp.1-12.

[4] Zimm C. and Boeder A., Design and performance of a permanent magnet rotary refrigerator, *International Journal of Refrigeration*, vol. 29, 2006, pp.1302-1306.

[5] Engelbrecht K., Nellis G., and Klein S., Predicting the performance of an active magnetic regenerator refrigerator used for space cooling and refrigeration, *HVAC&R Research*, vol. 12, 2006, pp.1077-1095.

[6] Siddikov B.M., Wade B.A., Schultz D.H., Numerical simulation of the active magnetic regenerator, *Computers&Mathematics with Applications*, Vol. 49, 2005, pp. 1525-1538.

[7] Sarlah A., Kitanovski A., Poredos A., Egolf P.W., Sari O., Gendre F., Besson Ch., Static and rotating active magnetic regenerators with porous heat exchangers for magnetic cooling, *International Journal of Refrigeration*, vol. 29, 2006, pp.1332-1339.

[8] Petersen T.F., Engelbrecht K., Bahl C.R.H, Elmegaard B., Pryds N. and Smith A., Comparison between a 1D and a 2D numerical model of an active magnetic regenerative refrigerator, *Journal of Physics D: Applied Physics*,vol. 41, 2008.

[9] Sarlah A. and Poredos A., Dimensionless numerical model for simulation of active magnetic regenerator refrigerator, *International Journal of Refrigeration*, vol. 36, 2010, pp.1061-1067.

[10] Roudaut J., Kedous-Lebouca A., Yonneta J.P., Muller C., *Numerical analysis of an active magnetic regenerator*, *International Journal of Refrigeration*, vol.34, 2011, pp.1797-1804.

[11] Eriksen D., Engelbrecht K., Bahl C.R.H., Bjørk R., Nielsen K.K, Insinga R.A., Pryds N., Design and experimental tests of a rotary active magnetic regenerator prototype, *International Journal of Refrigeration*, vol.58, 2015, pp. 14–21.

[12] Lozano J.A., Engelbrecht K., Bahl C.R.H., Nielsen K.K, Barbosa J.R., Prata A.T., Pryds N., Experimental and numerical results of a high frequency rotating active magnetic refrigerator, *International Journal of Refrigeration*, vol.37, 2014, pp.92-98.

[13] Chen Y.C., Qin L., Meng Z.H., Yang D.F., Wu C., Fu Z., Zheng Y.Z., Liu J.L, Tarasenko R., Orendáč M., Prokleška J., Sechovskýe V. and Tong M.L., Study of a magnetic-cooling material Gd(OH)CO3, *Journal of Materials Chemistry*, vol. 25, 2014, pp. 9851-9858.

[14] Vasile C. and Muller C., Innovative design of a magnetocaloric system, *International Journal of Refrigeration*, vol. 29, 2006, pp. 1318-1326.

[15] Shir F. and Mavriplis C., Analysis of room temperature magnetic regenerative refrigeration, *International Journal of Refrigeration*, vol. 28, 2005, pp. 616-627.

[16] Kobus C.J. and Wedekind G.L., An experimental investigation into natural convection heat transfer from horizontal isothermal circular disks, *International Journal of Heat and Mass Transfer*, vol. 44, 2001, pp. 3381-3384.

[17] Hassani A.V. and Hollands K.G., A simplified method for estimating natural convection heat transfer from bodies of arbitrary shape, *24th National Heat Transfer Conference*, Pittsburgh, Pennsylvania, 9-12 August, 1987.

[18] Kobus C.J. and Wedekind G.L., An experimental investigation into forced, natural and combined forced, and natural convection heat transfer from stationary isothermal circular disks, *International Journal of Heat and Mass Transfer*, vol. 38, 1995, pp. 3329-3339.